

Synthesis of tweezer type receptors for colorimetric detection of cyanide ions

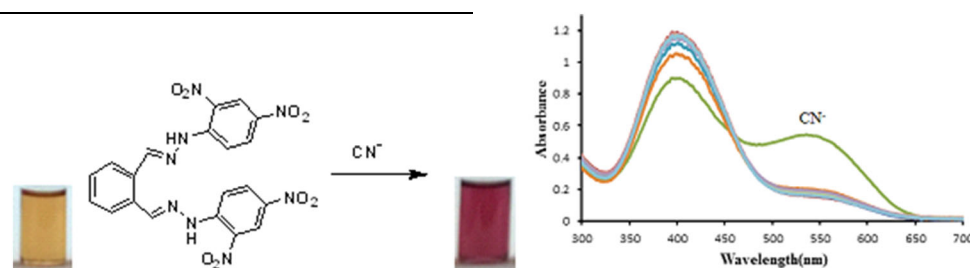
Priya Ranjan Sahoo¹ · Pragati Mishra¹ · Palak Agarwal¹ ·
Nikita Gupta¹ · Satish Kumar¹

Received: 20 October 2015 / Accepted: 5 January 2016
© Springer Science+Business Media Dordrecht 2016

Abstract Two tweezer type receptors based on the hydrazone functional group using *o*-phthalaldehyde moiety as spacer were synthesized and characterized via ¹H, ¹³CNMR, MALDI-MS and single crystal X-ray crystallographic techniques. The anion sensing abilities of the synthesized receptors were investigated in DMSO using UV–Visible spectroscopy and naked eye detection. The crystal structure revealed the presence of a DMSO molecule in the cavity of the receptor. A receptor displayed the formation of dark red color visible to the naked eye in the

presence of cyanide ions. The complex between the receptor and the cyanide ion proceeds through displacement of the DMSO molecule present in the cavity of the receptor. The stoichiometry of the complex between the receptor and the cyanide ion was determined by job's plot. The proton NMR spectroscopy and the DFT calculations were used to study the mechanism of the complex formation.

Graphical Abstract



Keywords Cyanide ion detection · Sensors · Hydrazone · Crystal structure · Optical recognition

Introduction

Ubiquitous anions play a prominent role in a variety of chemical and physical phenomena. Due to extensive use of anions in various industrial processes, there is widespread release of anions into the natural habitat as pollutants [1]. The abundance of highly toxic cyanide anion is extremely high in dyes, paints, herbicides and leather industry [2, 3].

✉ Satish Kumar
satish@ststephens.edu

¹ Department of Chemistry, St. Stephen's College, University Enclave, Delhi 110007, India

It is well known that the toxic cyanide ions act in the living organisms through coordination with iron present in the active site of an enzyme cytochrome c, which disrupt the electron transport chain in mitochondria, reducing the oxygen utilization and oxidative metabolism. There are evidences to support the claim that cyanide ions plays an important role in blocking cellular respiration to attack central nervous system [4, 5]. The unavoidable usages of cyanide ions in prominent fields like mineral processing, electroplating and gold industry further creates a need for CN^- detection and quantification [6, 7]. Cyanide contamination also originate from biological aspects [8]. In order to keep pace with industrial revolution, quick and easy detection of toxic anions particularly cyanide ions is extremely important for environmental protection and monitoring [1]. Therefore, there is a strong need for efficient probe for selective and sensitive detection of cyanide ions. The winds of anion sensing has strengthened from recent past under the banner of visual and optical responses and other methods [9, 10]. Visual detection of anion through distinct color change is quite simple and most noteworthy [11]. The detection of anionic species is dependent on hydrogen bonding and electrostatic interactions etc. [12]. The receptor-CN recognition relies on the ability of CN^- ion towards effective interaction with host molecule [13]. In order to ensure effective binding of anionic species with the receptor, the functional groups such as amines, amides, ureas and thioureas have already been incorporated into the structure of the synthetic receptors to achieve strong hydrogen bonding interactions [14–16].

Keeping the nucleophilicity concept of CN^- in mind, the research group led by Hong have designed coumarin based sensor for in vitro detection of CN^- species [17]. The other groups led by Yoon have also developed mono and di aldehyde based hydroxyl fluorescein probes for cyanide recognition [18, 19]. They have also injected the DMSO solution of the probe into the lungs of mice in order to image cyanide inside the mice body. The reported sensing probes also include dipyrrole carboxamide [20], azo phenyl thiourea [21], disperse orange-3 derivative [22], substituted *N*-nitrophenyl benzamide [23], nitro azo salicylaldehyde [24], dipyrrole derivatives [25] and *N*-acyl triazene scaffolds [26].

To induce anion coordination to the synthetic receptors, it is necessary to maximize the polarizing tendency of the N–H group of the receptor, which can be achieved through the electron withdrawing groups like $-\text{NO}_2$ to enhance the anion coordination ability.

In this article, we present the synthesis and evaluation of colorimetric sensor for cyanide ion, which possess hydrazone groups with $-\text{NO}_2$ substituents. The sensor was observed to be selective for cyanide ions in DMSO. The

effect of nitro groups in anion coordination and the cage effect using DFT studies were also evaluated.

Experimental

Reagents

All the reagents *o*-phthalaldehyde, 2, 4-dinitro phenyl hydrazine, 4-nitrophenyl hydrazine, THF and acetic acid were purchased from spectrochem, India. All the tetrabutyl ammonium salts of various anions were purchased from CDH AR grade.

Instruments

The NMR spectra were recorded on a 400 MHz Jeol spectrometer. The IR spectrum was recorded on a Perkin Elmer FT-IR-RXI spectrometer. Elemental analysis was performed on elemental analysensysteme Germany Vario Micro Cube CHNSO system at USIC facility. Single crystal data was recorded on an Oxford Diffraction, X-caribur-S single crystal XRD machine.

UV–Visible studies

A 1.0 mL solution of chelator **1** (2.5×10^{-5} M) was prepared in a quartz cuvette and 1.0 mL of different anions (2.5×10^{-5} M) were mixed well and the UV visible spectrum was recorded on an Ocean Optics USB4000 UV–Visible spectrometer.

Computations

Calculations reported in this paper were performed using Gaussian 09 program [27]. The initial geometry of the receptor **2** was generated using Gaussview 5.0 program [27]. The geometries generated using Gaussview were optimized using DFT/B3LYP/6-31G(d) method. The local minimum for the optimized structure was confirmed through absence of negative frequency. The time dependent DFT method was used to obtain the transition energy and absorption spectra.

Synthesis

Synthesis of receptor 1

In a round bottom flask (150 mL), *o*-phthalaldehyde (0.5 g, 3.73 mmol) and 4-nitrophenyl hydrazine (1.26 g, 8.28 mmol) were dissolved in THF (10 mL). The mixture was warmed over heating mantle and kept for 15–20 min

followed by the addition of 2–3 drops of acetic acid. The precipitates were filtered and washed with little THF. The product was purified through recrystallization using THF and dried. Yield 0.64 g m.pt. 238–240 °C. FT-IR (KBr, ν/cm^{-1}): 3450, 2928, 2852, 1642, 1390 and 1086. $^1\text{H-NMR}$ (400 MHz, DMSO-d_6): $\delta = 11.45$ (s, 2H), 8.51 (s, 2H) 8.14 (d, 4H, $J = 8.4$ Hz), 7.86 (dd, 4H, $J = 6$ Hz) 7.43 (dd, 4H, $J = 6$ Hz), 7.19 (d, 2H, $J = 8.4$ Hz). $^{13}\text{C-NMR}$ (100 MHz, DMSO-d_6): $\delta = 150.5, 140.7, 138.6, 132.25, 129.5, 127.8, 126.2, 111.5$. MALDIMS: $m/z =$ Calculated 404.1233; found $[\text{M}+1]^+$: 405.0601. $\text{C}_{20}\text{H}_{16}\text{N}_6\text{O}_4$ CHN % Calcd. C: 59.30, H: 3.99, N: 20.78; found C: 59.53, H: 3.92, N: 20.03.

Synthesis of receptor 2

In a round bottom flask (150 mL), *o*-phthalaldehyde (0.5 g, 3.73 mmol) and 2, 4-dinitrophenylhydrazine (1.26 g, 8.28 mmol) were dissolved in 10 mL THF. The reaction mixture was warmed and kept for 15–20 min followed by the addition of 2–3 drops of acetic acid. The precipitated product was filtered followed by washing with small amount of THF. The product was recrystallized twice with THF and dried to give yellow-orange product. Yield 0.54 g. m.pt: 230–232 °C FT-IR (KBr, ν/cm^{-1}): 2922, 2852, 1740, 1615, 1581, 1462, 1333, 1264, 1139, 992, 908, 720. $^1\text{H-NMR}$ (400 MHz, DMSO-d_6): $\delta = 11.8$ (s, 1H) 9.9 (brs, 2H), 9.19 (s, 1H) 8.9 (s, 1H), 8.4–8.0 (m, 8H), 7.6–7.5 (m, 1H). MALDI-MS: $m/z =$ Calculated 496.1013; found $[\text{M}]^+$: 496.2639 $[\text{M}+\text{Na}]$: 517.2861; $\text{C}_{20}\text{H}_{14}\text{N}_8\text{O}_8$ CHN% Calcd. C: 48.59, H: 2.85, N: 22.67; found C: 49.00, H: 2.88, N: 22.37.

Result and discussion

Crystallographic studies

The receptors were synthesized as per the Scheme 1 in moderate to high yield and characterized by IR, NMR, Mass and elemental analyses. Single crystals of receptor 2 suitable for data collection were grown through slow evaporation method. The asymmetric unit in the crystal structure of the receptor 2 is solvated by two solvent

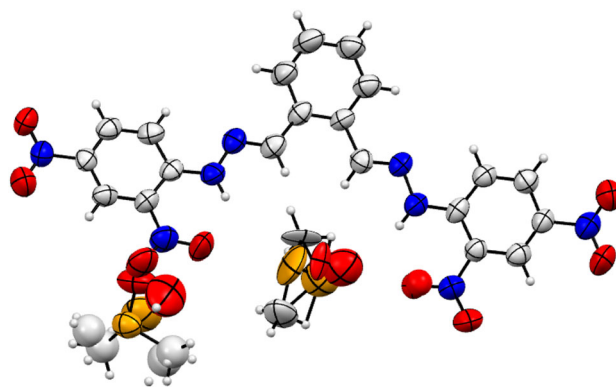


Fig. 1 ORTEP [28] view of crystal structure of receptor 2 with displacement ellipsoids at the 50 % probability level (CCDC 1416520)

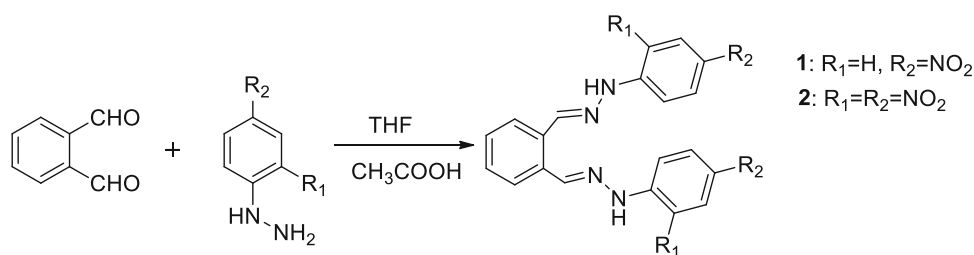
Table 1 Hydrogen-bond geometry (Å, °)

<i>D</i> — <i>H</i> ... <i>A</i>	<i>D</i> — <i>H</i>	<i>H</i> ... <i>A</i>	<i>D</i> ... <i>A</i>	<i>D</i> — <i>H</i> ... <i>A</i>
N005—H005...O2	0.86	2.00	2.56 (5)	122.1
N005—H005...O2A	0.86	2.00	2.619 (9)	128.1
N008—H008...O00E	0.86	1.99	2.603 (6)	127.2
C00O—H00O...O00G ⁱ	0.93	2.54	3.416 (7)	157.1
C00Q—H00Q...O004 ⁱⁱ	0.93	2.50	3.418 (7)	167.5
C00V—H00V...O013 ⁱⁱⁱ	0.93	2.38	3.240 (9)	153.3
C00V—H00V...S0 ⁱⁱⁱ	0.93	2.84	3.562 (18)	135.2
C00V—H00V...O0 ⁱⁱⁱ	0.93	2.66	3.32 (5)	128.8
C015—H01C...O00D ^{iv}	0.96	2.62	3.411 (9)	139.7
C015—H01C...N00F ^{iv}	0.96	2.53	3.263 (9)	133.3
C3—H3C...O009 ^v	0.96	2.63	3.549 (18)	159.5
C3A—H3AC...O3A ^{vi}	0.96	2.46	3.23 (4)	137.3

Symmetry codes (i) $x + 1, y, z - 1$; (ii) $x - 1, y, z + 1$; (iii) $x, -y + 1/2, z + 1/2$; (iv) $x, -y + 1/2, z - 1/2$; (v) $x - 1, y, z$; (vi) $-x, -y + 1, -z + 1$

(DMSO) molecules (Fig. 1). One solvent molecule DMSO occupies the cavity of the receptor while another DMSO solvent molecule resides closer to the nitro group and is coordinated through weak intermolecular interactions. Two intramolecular N—H...O hydrogen bonds are present in the asymmetric unit. The structure is characterized by several short intermolecular and intramolecular hydrogen bonds

Scheme 1 The synthesis route of the receptor 1 and 2



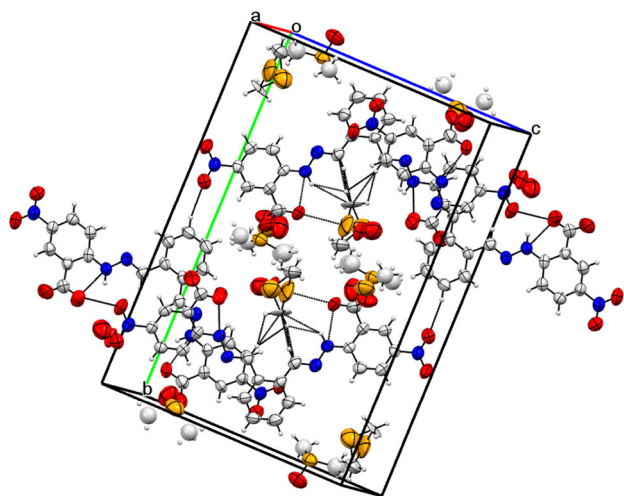


Fig. 2 Crystal packing diagram of receptor **2** viewed along *axis b* showing intermolecular short contacts. Ellipsoids are shown at 50 % probability level

(Table 1). The crystal packing diagram (Fig. 2) suggested that the solvent molecule occupies the space between the layers of the receptor molecule. The solvent molecules were bound to the receptor molecules through short intermolecular H-bonds involving oxygen atom of the DMSO and H-atoms connected to the nitrogen. Two nitroaromatic units are at 101.08° dihedral angle to each other. The two DMSO solvent molecules were highly disordered and modeled using SIMU, FREE and EADP instructions.

Naked eye detection

The synthesized receptors were explored for colorimetric response towards different anions in DMSO. In order to evaluate the anion binding preference, standard solutions of the receptors **1** and **2** (1×10^{-4} M) were prepared in DMSO. UV–Visible spectral variation experiments in the presence of **1** equivalent of different anions were performed: No color change was observed with receptor **1** in the presence of different anionic species (Fig. 3). It was observed that the addition of **1** equivalent cyanide ions to a solution of receptors **2** in DMSO produced a visible change in color along with spectral variation while no spectral

variations or color change to the naked eye was observed with other anions (Fig. 4).

UV–Visible studies

UV–Visible spectra indicates that the receptor **2** absorb at 400 nm with a small shoulder peak at 540 nm. The presence of a small absorption band at 540 nm indicates the formation of an inclusion complex between DMSO and receptor **2**. The absorption band at 540 nm was not observed in the spectrum of receptor **2** in THF. The formation of receptor **2**-DMSO inclusion complex was also supported by X-ray crystallographic studies, which indicates that the DMSO molecule occupies the receptor **2** cavity (Fig. 1). The absorption peak at 400 nm decreased in intensity and 540 nm increased in intensity on the addition of one equivalent of cyanide ion, which indicated that the complex between cyanide ions and the receptor **2** is stronger than the complex between DMSO and receptor **2**. Further, the **2** – CN complex is formed through displacement of DMSO molecule. Other interfering anions such as F^- , OAc^- did not show any change on the absorbance profile indicating the selectivity of receptor **2** towards CN^- ion which produced a clearly visible deep red color from an orange solution. The respective variation in absorbance with respect to different anions is depicted in the Fig. 5. However, the receptor **1** did not respond to the presence of any of the anions tested. It is pertinent to note that the only difference between receptor **1** and **2** is the number of nitro groups which suggests the important role nitro groups play in the recognition process. In addition, the fact that receptor **2** selectively recognize, a more nucleophilic and less basic cyanide ion in comparison to the fluoride or other anion suggest that pK_a (pK_a : [29] $F = 15$, $CN = 12.9$, $OAc = 12.6$, $Cl = 1.8$, $Br = 0.9$) of anion is not solely responsible for the observed selectively, other factors such as size, geometry and nucleophilicity of the anions are also important (Figs. 6, 7).

The two nitro groups played a key role in better charge separation in comparison to a single nitro group due to which color changed from yellow to red [30] as reported in the literature which also suggests that nitro group plays an important role in anion coordination [31]. Anion binding



Fig. 3 Colour change on the addition of 1.0 equivalent of tetrabutyl ammonium anions into a solution of receptor **1** in DMSO. $[1] = 5.0 \times 10^{-5}$. From left to right; A = Free receptor, B = CN^- , C = F^- , D = OAc^- , E = Cl^- , F = Br^- , G = I^- , H = NO_3^- , I = $H_2PO_4^-$, J = HSO_4^-



Fig. 4 Color change on the addition of 1.0 equivalent of tetrabutyl ammonium anions into a solution of receptor **2** in DMSO. $[2] = 5.0 \times 10^{-5}$. From left to right; A = Free receptor,

B = CN^- , C = F^- , D = OAc^- , E = Cl^- , F = Br^- , G = I^- , H = NO_3^- , I = H_2PO_4^- , J = HSO_4^- , K = PF_6^- , L = PhO^-

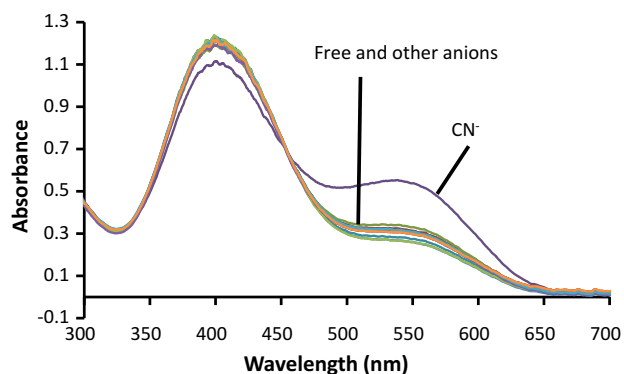


Fig. 5 Absorption spectra of **2** ($[2] = 2.5 \times 10^{-5}$ M) with 1.0 equivalent of *n*-butyl ammonium salt of various anions ($[\text{F}^-]$, $[\text{Cl}^-]$, $[\text{Br}^-]$, $[\text{I}^-]$, $[\text{HSO}_4^-]$, $[\text{H}_2\text{PO}_4^{2-}]$, $[\text{PF}_6^-]$, $[\text{NO}_3^-]$, $[\text{OAc}^-]$, $[\text{PhO}^-] = 2.5 \times 10^{-5}$ M) in DMSO. For simplicity spectra of only few important anions are shown

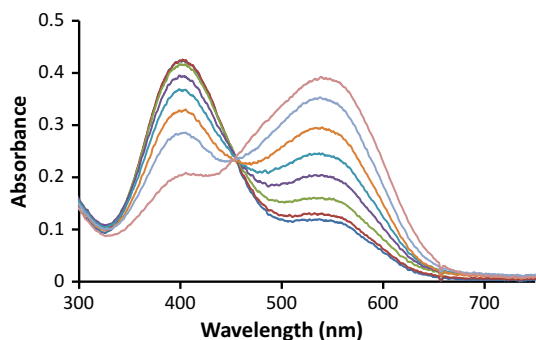


Fig. 6 UV-Vis spectrum of the receptor **2** ($[2] = 2.5 \times 10^{-5}$ M) in the presence of cyanide ions ($[\text{CN}^-] = 0-4.12 \times 10^{-5}$ M) in DMSO

was also attributed to H-bond interactions [23]. The binding sites containing highly polarized N-H group were also reported for recognition of anions [32]. The highly polarized group may deprotonate in the presence of anions, which causes substantial electron delocalization and ultimately produce a different absorption spectral band and the visual color change [33].

In order to further understand the binding process, a titration experiment was performed. Upon gradual addition of a solution of cyanide ion solution in DMSO to a solution of receptor **2** in DMSO, the absorption peak at 400 nm gradually decreased and a peak at 550 nm appeared. A clearly distinguishable isosbestic point was observed at 451 nm. The distinct isosbestic point confirmed the

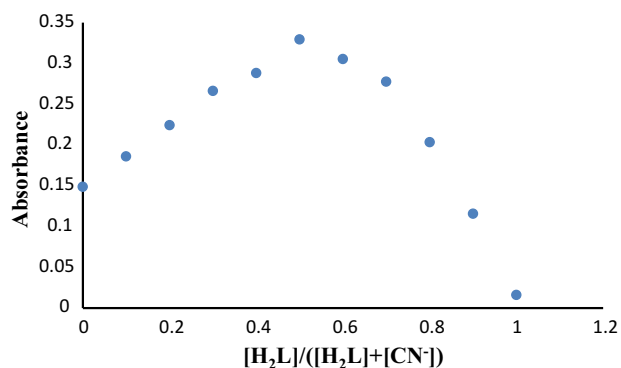


Fig. 7 Job's plot between receptor **2** and CN^- ion in DMSO. Absorbance at 499 nm was plotted as a function of the molar ratio $[\text{H}_2\text{L}]/([\text{H}_2\text{L}]+[\text{CN}^-])$

formation of a stable complex between the receptor **2** and CN^- . A reasonable bathochromic shift of 135 nm was experienced during complex formation. Finally, the color changed from yellow to dark red. The stoichiometry of the complex was confirmed through Job's plot, which indicated it to be 1:1. No such characteristics were observed in the case of other anions.

In order to determine the binding strength of receptor towards CN^- ions, binding affinity studies were performed using Hypspec [34]. When the results were analyzed using Hypspec, a $\log\beta$ value of 4.7527 ± 0.0013 was obtained indicating a strong complex between cyanide ions and the receptor **2** in DMSO.

In order to obtain the detection limit of the synthesized receptor **2** towards cyanide ion, UV-Visible absorbance was plotted against the cyanide ion concentration. A linear change in the absorbance intensity with increasing cyanide ion concentration was obtained (Fig. 8), which was used for calculation of detection limit based on $3\sigma/m$, where σ is the standard deviation and m is the slope of the intensity versus cyanide concentration plot. A detection limit of UV-Visible spectrophotometry was obtained as $1.4 \mu\text{M}$ which is less than the WHO prescribed limit for cyanide ion as $1.9 \mu\text{M}$.

NMR studies

To investigate the mechanism of complex formation between the cyanide ion and the receptor **2**, the NMR

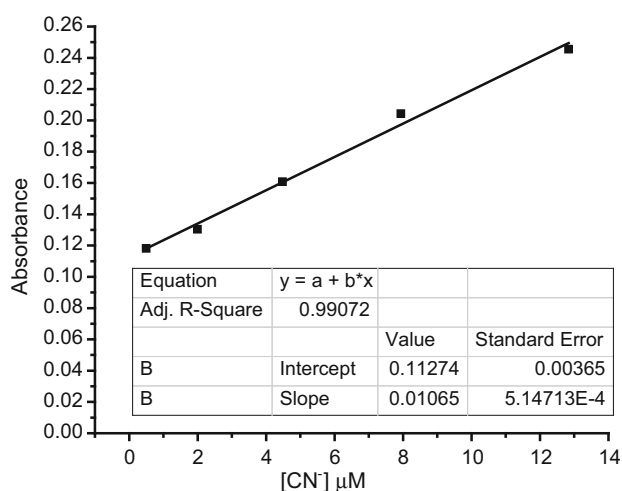


Fig. 8 Determination of detection limit of receptor **2** for cyanide ion at 547 nm

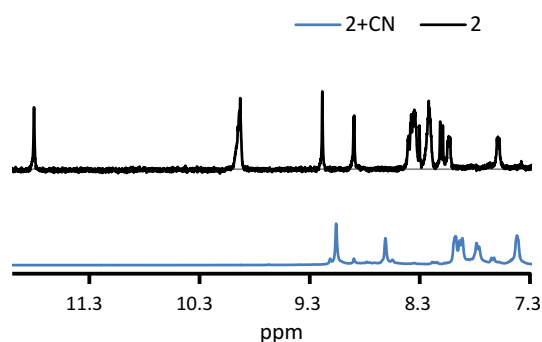


Fig. 9 $^1\text{H-NMR}$ spectra of receptor **2** [**2**] = 60 mM and **2** + CN (cyanide ions 1.0 eq.) in DMSO- d_6

spectra of receptor **2** and receptor **2** + CN ions in DMSO- d_6 were recorded (Fig. 9). It was observed that the NH group signal appeared at δ 11.80 and δ 9.19 in proton NMR spectra of receptor **2**. The proton NMR signal of NH proton disappeared at δ 11.80 while the other N–H signal at δ 9.19 shifted to lower ppm value when cyanide ions were added to the receptor **2** in DMSO- d_6 . The NMR indicates that the receptor **2** detect cyanide ions through deprotonation process which resulted in color change.

Computational studies

In order to further understand the binding process at the molecular level, density functional theory was used [35]. Calculations were performed at B3LYP/6-31G(d) level as they have been used to predict the properties of such systems successfully. Various conformers of the receptor **2** were optimized. The conformer shown in Fig. 10a was

found to be the most stable (Table 2). Rotation of nitroaromatic group or the CN group destabilized the structure. The same conformer was also observed in single crystal X-ray crystallographic studies. Therefore, anion binding studies were also performed using the same conformers. Various binding modes were optimized to provide the lowest energy complex geometry shown in Fig. 10c–f (Table 2) using B3LYP/6-31G(d) method. The geometry shown in Fig. 10d provided the lowest energy among all the binding modes. The presence of two cyanide ions per receptor **2** molecule was observed to be sterically unfavourable. The structure shown in Fig. 10d was observed to be more stable by -99.23 kcal/mol [$\Delta E = E_{\text{complex}} - E_{\text{CN}} - E_{(2)}$] in comparison to the free receptor **2** and cyanide ion combined energy indicating that the stability of the complex. Further, the solvation energy of the receptor **2** and **2** + CN complex was calculated in DMSO (Table 2). It was observed that the receptor **2** was more solvated than the complex, indicating that the solvent interact with the receptor **2** through H-bond interactions. The formation of a complex between cyanide ions and the receptor **2** reduces this interaction due to the presence of HCN in the receptor cavity. To further investigate the observed bathochromic shift in UV–Visible spectra on the addition of cyanide ions, time-dependent DFT studies using 6-31G(d) basis set were performed using the Gaussian 09 software suite. The Table 3 lists various parameters calculated for electronic transition using TD-DFT/6-31G(d) in receptor **2** and **2** + CN complex. The singlet excitations in receptor **2** were mainly contributed by HOMO to LUMO (S_0 to S_1) and HOMO to LUMO+2 (S_0 to S_3) orbitals. The energy (2.87 eV, 432 nm) of HOMO to LUMO+2 transition (S_0 to S_3) is close to the observed absorption maxima in DMSO (Table 3; Fig. 11). The total change in dipole moment was determined to be 30.07 debye, which indicated deprotonation of N–H and generation of high negative charge in the receptor **2** as suggested by NMR data [36]. Similarly, the transition between HOMO to LUMO (S_0 to S_1) and HOMO to LUMO+1 (S_0 to S_2) orbitals contribute mainly to the singlet excitation in the **2** – CN complex. The energy (2.18 eV, 568 nm) for the transition between HOMO to LUMO+1 is close to the observed maxima in DMSO (Table 3; Fig. 11). The bathochromic shift observed during the complex formation between cyanide ions and the receptor **2** can be explained by comparing the calculated singlet excitation energy observed in **2** – CN complex and the receptor **2**. A small singlet excitation energy in the **2** – CN complex indicates a bathochromic shift. Further, the cyanide binding to the receptor **2** leads to the delocalization of electron density in receptor **2** causing bathochromic shift (Fig. 11).

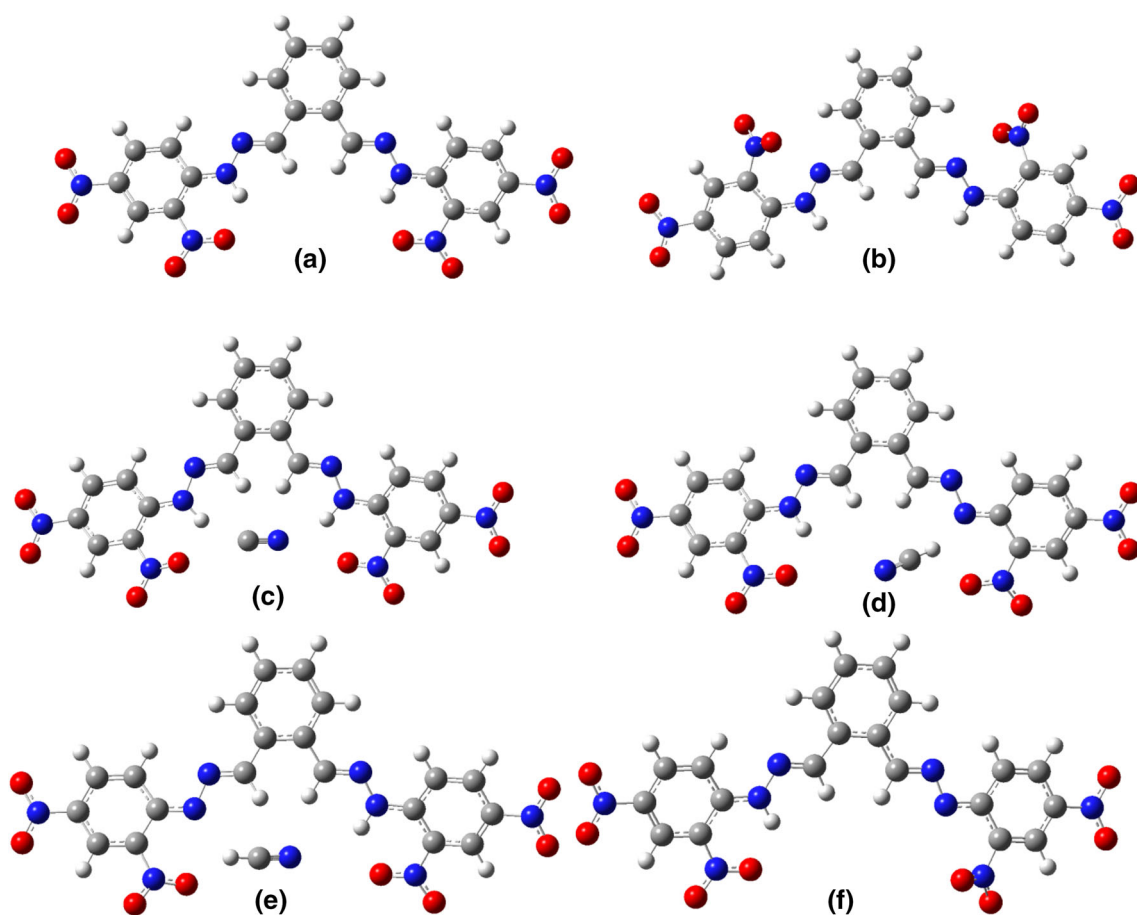


Fig. 10 The B3LYP/6-31G(d) optimized geometries of **a** receptor **2** and **2** – CN complex modes between receptor **2** and cyanide ion

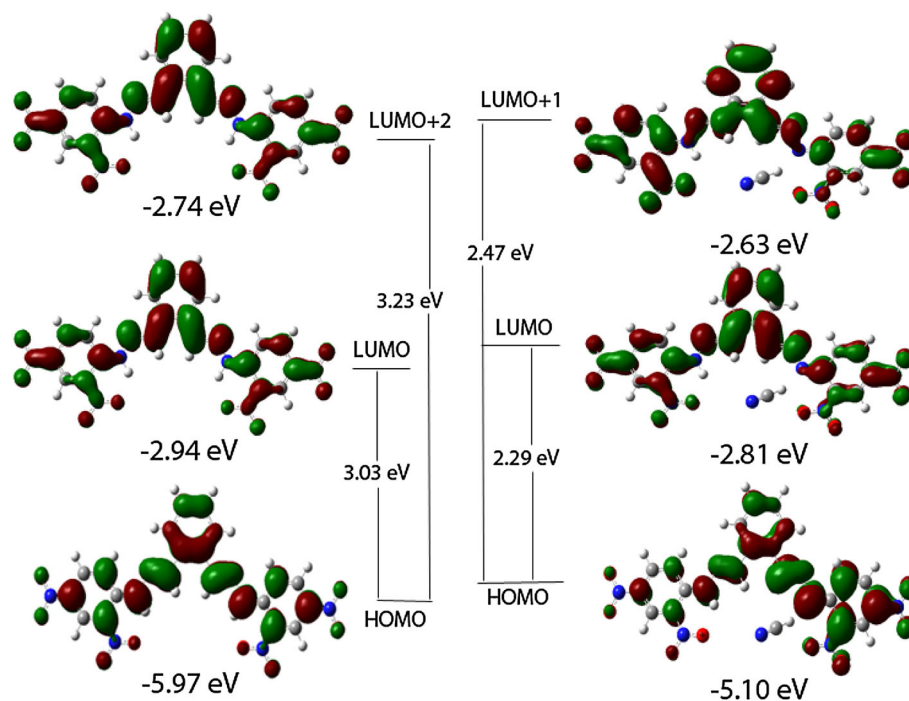
Table 2 The energy of the receptor **2** and **2** + CN calculated using DFT/B3LYP/6-31G(d) method

Structure	Energy (Hartree)	Energy (kcal/mol)	ΔG_{solv} (kcal/mol), DMSO
9a	-1809.92194505	-1,135,742.31	-15.92
9b	-1809.88526064	-1,135,719.29	
9c	-1902.82,646,010	-1,194,040.73	
9d	-1902.90461024	-1,194,089.77	0.0009
9e	-1902.84196484	-1194050.46	
9f	-1809.39721827	-1,135,413.04	

Table 3 Electronic excitation parameters for receptor **2** and **2** + CN complex obtained using TD-DFT/6-31G(d) method

Receptor	CIC	E(eV)[λ (nm)]	μ_x	μ_y	μ_z	μ_{total}	f	
2	S_0 to S_1	H to L (0.69)	2.59 (478.86)	7.92	0.00	-0.17	24.68	0.6161
	S_0 to S_2	H to L + 1 (0.69)	2.72 (455.42)	0.00	-2.50	0.00	4.82	0.1265
	S_0 to S_3	H to L + 2 (0.69)	2.87 (431.90)	8.74	0.00	0.21	30.07	0.8323
2 + CN	S_0 to S_1	H to L (0.70)	1.96 (632.89)	-3.97	-0.23	0.16	6.23	0.1178
	S_0 to S_2	H to L + 1 (0.70)	2.18 (568.21)	5.86	-0.77	0.05	13.72	0.2887

Fig. 11 Energy diagrams for main orbitals of **2** and **2** – CN complex calculated using the DFT/B3LYP/6-31G method



Conclusion

In conclusion, we have reported the design and synthesis of two simple hydrazone based tweezer type receptors for cyanide ions. The receptor produced selective and sensitive colorimetric response towards cyanide ions visible to the naked eye as well as the distinct absorbance change in UV–Vis spectra. A single isosbestic point was observed in the cyanide titration profile. The job's plot also confirmed 1:1 complex stoichiometry between cyanide ions and the receptor **2**. The binding titration experiment using Hypspec package also confirmed strong binding affinity of the receptor **2** for CN^- ions. The mechanism of complexation was investigated using DFT and NMR experiments, which confirmed that the complex formation involve N-H proton abstraction by cyanide ions.

Acknowledgments Authors sincerely thank UGC (No.41-235/2012) and DST (No. SR/FT/CS-054/2012), New Delhi, India for financial support. Authors are thankful to the Director, USIC University of Delhi for instrumental facilities. The authors are also thankful to the Principal, St. Stephen's College for providing the necessary infrastructure.

References

- Gale, P.A., Caltagirone, C.: Anion sensing by small molecules and molecular ensembles. *Chem. Soc. Rev.* **44**, 4212–4227 (2015)
- Li, Q., Zhang, J.-H., Cai, Y., Qu, W.-J., Gao, G.-Y., Lin, Q., Yao, H., Zhang, Y.-M., Wei, T.-B.: A facile colorimetric and fluorescent cyanide chemosensor: utilization of the nucleophilic addition induced by resonance-assisted hydrogen bond. *Tetrahedron* **71**(5), 857–862 (2015)
- Ravikanth, M., Dvivedi, A., Rajakannu, P.: Meso-salicylaldehyde substituted BODIPY as chemodosimetric sensor for cyanide anion. *Dalton Trans.* **44**, 4054–4062 (2015)
- Ashton, T.D., Jolliffe, K.A., Pfeffer, F.M.: Luminescent probes for the bioimaging of small anionic species in vitro and in vivo. *Chem. Soc. Rev.* **44**, 4547–4595 (2015)
- Hu, J., Li, J., Qi, J., Sun, Y.: Selective colorimetric and “turn-on” fluorimetric detection of cyanide using an acylhydrazone sensor in aqueous media. *New J. Chem.* **39**, 4041–4046 (2015)
- Mudder, T., Botz, M.: Cyanide and society: a critical review. *Ejmp Ep* **4**(1), 62–74 (2004)
- Isaad, J., El Achari, A.: A novel glycoconjugated *N*-acetyl amino aldehyde hydrazone azo dye as chromogenic probe for cyanide detection in water. *Anal. Chem. Acta* **694**(1), 120–127 (2011)
- Wang, F., Wang, L., Chen, X., Yoon, J.: Recent progress in the development of fluorometric and colorimetric chemosensors for detection of cyanide ions. *Chem. Soc. Rev.* **43**(13), 4312–4324 (2014)
- You, L., Zha, D., Anslyn, E.V.: Recent Advances in Supramolecular Analytical Chemistry Using Optical Sensing. *Chem. Rev* (2015)
- Kwon, H., Jiang, W., Kool, E.T.: Pattern-based detection of anion pollutants in water with DNA polyfluorophores. *Chem. Rev.* **6**(4), 2575–2583 (2015)
- Lee, H.J., Park, S.J., Sin, H.J., Na, Y.J., Kim, C.: A selective colorimetric chemosensor with an electron-withdrawing group for multi-analytes CN^- and F^- . *New J., Chem* (2015)
- Dalapati, S., Jana, S., Guchhait, N.: Anion recognition by simple chromogenic and chromo-fluorogenic salicylidene Schiff base or reduced-Schiff base receptors. *Spectrochim. Acta A* **129**, 499–508 (2014)
- Zhang, C., Liu, C., Li, B., Chen, J., Zhang, H., Hu, Z., Yi, F.: A new fluorescent “turn-on” chemodosimeter for cyanide based on dual reversible and irreversible deprotonation of NH and CH groups. *New J. Chem* (2015)

14. Xu, Z., Chen, X., Kim, H.N., Yoon, J.: Sensors for the optical detection of cyanide ion. *Chem. Soc. Rev.* **39**(1), 127–137 (2010)
15. Kaur, N., Dhaka, G., Singh, J.: Simple naked-eye ratiometric and colorimetric receptor for anions based on azo dye featuring with benzimidazole unit. *Tetrahedron Lett.* **56**, 1162–1165 (2015)
16. Robbins, T.F., Qian, H., Su, X., Hughes, R.P., Aprahamian, I.: Cyanide detection using a triazolopyridinium salt. *Org. Lett.* **15**(10), 2386–2389 (2013)
17. Lee, K.-S., Kim, H.-J., Kim, G.-H., Shin, I., Hong, J.-I.: Fluorescent chemodosimeter for selective detection of cyanide in water. *Org. Lett.* **10**(1), 49–51 (2008)
18. Kwon, S.K., Kou, S., Kim, H.N., Chen, X., Hwang, H., Nam, S.-W., Kim, S.H., Swamy, K., Park, S., Yoon, J.: Sensing cyanide ion via fluorescent change and its application to the microfluidic system. *Tetrahedron Lett.* **49**(26), 4102–4105 (2008)
19. Nam, S.-W., Chen, X., Lim, J., Kim, S.H., Kim, S.-T., Cho, Y.-H., Yoon, J., Park, S.: In vivo fluorescence imaging of bacteriogenic cyanide in the lungs of live mice infected with cystic fibrosis pathogens. *PLoS One* **6**(7), e21387 (2011)
20. Chen, C.-L., Chen, Y.-H., Chen, C.-Y., Sun, S.-S.: Dipyrrole carboxamide derived selective ratiometric probes for cyanide ion. *Org. Lett.* **8**(22), 5053–5056 (2006)
21. Gimeno, N., Li, X., Durrant, J.R., Vilar, R.: Cyanide sensing with organic dyes: studies in solution and on nanostructured Al₂O₃ surfaces. *Chem. Eur. J.* **14**(10), 3006–3012 (2008)
22. Niu, H.-T., Jiang, X., He, J., Cheng, J.-P.: A highly selective and synthetically facile aqueous-phase cyanide probe. *Tetrahedron Lett.* **49**(46), 6521–6524 (2008)
23. Sun, Y., Wang, G., Guo, W.: Colorimetric detection of cyanide with *N*-nitrophenyl benzamide derivatives. *Tetrahedron* **65**(17), 3480–3485 (2009)
24. Lee, K.-S., Lee, J.T., Hong, J.-I., Kim, H.-J.: Visual detection of cyanide through intramolecular hydrogen bond. *Chem. Lett.* **36**(6), 816–817 (2007)
25. Ding, Y., Li, T., Zhu, W., Xie, Y.: Highly selective colorimetric sensing of cyanide based on formation of dipyrin adducts. *Org. Biomol. Chem.* **10**(21), 4201–4207 (2012). doi:10.1039/c2ob25297j
26. Chung, Y., Ahn, K.H.: *N*-acyl triazenes as tunable and selective chemodosimeters toward cyanide ion. *J. Org. Chem.* **71**(25), 9470–9474 (2006)
27. Frisch, M.J., Trucks, G.W., et al.: Gaussian 09, Revision A02. Gaussian, Inc, Wallingford (2009)
28. Macrae, C.F., Bruno, I.J., Chisholm, J.A., Edgington, P.R., McCabe, P., Pidcock, E., Rodriguez-Monge, L., Taylor, R., Streek, J.V., Wood, P.A.: Mercury CSD 2.0—new features for the visualization and investigation of crystal structures. *J. Appl. Cryst.* **41**(2), 466–470 (2008)
29. Taft, R.W., Bordwell, F.G.: Structural and solvent effects evaluated from acidities measured in dimethyl sulfoxide and in the gas phase. *Acc. Chem. Res.* **21**(12), 463–469 (1988). doi:10.1021/ar00156a005
30. Zhu, X., Lin, Q., Lou, J.-C., Lu, T.-T., Zhang, Y.-M., Wei, T.-B.: Colorimetric probes designed to provide high sensitivity and single selectivity for CN⁻ in aqueous solution. *New J. Chem.* **39**(9), 7206–7210 (2015). doi:10.1039/c5nj01158b
31. Kim, D.-S., Chung, Y.-M., Jun, M., Ahn, K.H.: Selective colorimetric sensing of anions in aqueous media through reversible covalent bonding. *J. Org. Chem.* **74**(13), 4849–4854 (2009)
32. Park, J., Kang, J.: A new colorimetric anion sensor which have both a fat brown RR dye and a nitrophenyl group as signaling group. *J. Incl. Phenom. Macrocycl. Chem.* **69**(1–2), 57–61 (2011). doi:10.1007/s10847-010-9813-5
33. Choi, Y., Kang, J.: Chromogenic anion receptors based on 4-nitrophenylhydrazone and phenylhydrazone. *J. Incl. Phenom. Macrocycl. Chem.* **79**(1–2), 95–102 (2014). doi:10.1007/s10847-013-0328-8
34. Gans, P., Sabatini, A., Vacca, A.: Investigation of equilibria in solution. Determination of equilibrium constants with the HYPERQUAD suite of programs. *Talanta* **43**(10), 1739–1753 (1996)
35. Satheskumar, A., El-Mossalamy, E.H., Manivannan, R., Parthiban, C., Al-Harbi, L.M., Kosa, S., Elango, K.P.: Anion induced azo-hydrazone tautomerism for the selective colorimetric sensing of fluoride ion. *Spectrochim. Acta A* **128**, 798–805 (2014). doi:10.1016/j.saa.2014.02.200
36. Nelson Jr, R.D., Lide Jr, D.R., Maryott, A.A.: Selected values of electric dipole moments for molecules in the gas phase. In: DTIC Document, (1967)